Composite tube behavior under low velocity impact

Giangiacomo Minak, Daniele Ghelli, Riccardo Panciroli,
Andrea Zucchelli

Alma Mater Studiorum – Università di Bologna, Mechanical Engineering
Department DIEM, Bologna – Italy

Abstract

Advanced applications of tubes made of carbon-epoxy composites in which the main external load is torque, have been recently developed in the industrial and sports fields.

In order to use these high specific performance material components, a fundamental problem for the designer is the low energy and velocity impact behavior. In fact such load events are very common during normal service life and their real effects on in-service component behavior are not well understood.

In the present work the results of an experimental test campaign performed with the aim of evaluating the mechanical behavior of tubular structures under impact, with and without torsional pre-load, are presented. In particular, the aspects on which the research was focused are the stacking sequence and the pre-load level, that proved to be a key factor for the impact response of the material. A numerical model based on the Ansys software was developed to describe the material behavior up to the first load drop.

Keywords: composites, carbon fiber, epoxy matrix, tubes, impact.

1 Introduction

Laminated composite materials, consisting of a polymer matrix reinforced by long carbon fiber, possess excellent mechanical properties (specific stiffness and strength, for example) when loaded in their plane but can be easily damaged by impact loads, such as those caused by accidental collisions during the production, operation or maintenance phases [1]. By virtue of their mechanical properties and despite their high cost, these materials have recently been used to produce components in the form of tubes such as high speed shafts for power transmission in paper industry machines or in high-performance applications and sports (masts and winches in sailboats, fishing rods, etc.).

While the international research on the impact on composite laminated plates includes many different contributions, including some by the authors of this paper [2–4], the phenomenon of side impact on tubes was studied only to a limited extent in recent years in the scientific literature, by analytical models [5, 6], numerical models [7–9] or experimentally [10].

In particular, the studies by Christoforou *et al.* [5] and Christoforou and Swanson [6] are focused on the dynamic response of the pipe, which takes account of the damage with simple analytical models. An exhaustive investigation conducted by means of a parametric finite element model was carried out by Krishnamurthy *et al* [7]. The parameters considered in this work are impactor mass and velocity, stacking sequence and boundary conditions, and their effect on the damage of the matrix and the magnitude of delaminated area, assessed with appropriate criteria from the calculated stresses, are determined. Using methods similar to those of the previous work, Kim *et al* [8] and Her and Liang [9] numerically investigated the effect of the stacking sequence and of the curvature on the dynamic response and damage in sequences comparable with those used in this memory. Finally, Doyum and Altay [10] focused on damage caused in glass-epoxy tubes by non-instrumented impacts of energy comparable to the energy of the present study, but on markedly different stacking sequences.

The final aim of this research is the determination of residual resistance to twisting of tubular composite structures subjected to lateral low velocity impacts. In this part, the results of impact tests performed considering different lay-ups and different conditions of pre-loading in torsion are discussed. The interpretation of the experimental results was assisted by a suitable non linear FEM model.

2 Materials and methods

The tubes considered, 200 mm long, 50 mm inside diameter and thickness 2.55 mm, were produced in an autoclave by overlapping 16 unidirectional plies of epoxy matrix reinforced with 60% in volume of T300 carbon fiber. Different lay-ups were utilized, two cross-ply listed as CP and two quasi-isotropic mentioned as QI (see Table 1 where the direction of 0º was cylinder generatrix one). As can be seen, there are two symmetrical lay-ups (CPS and QIS) and two non-symmetrical ones (CPNS and QINS).

Table 1: Stacking sequences.

label	lay-up
CPS	$[45/\text{-}45]_{4s}$
CPNS	$[45/\text{-}45]_8$
QIS	$[0_2/45/\text{-}45/45/\text{-}45/90_2]_s$
QINS	$[0_2/45/\text{-}45/45/\text{-}45/90_4/45/\text{-}45/45/\text{-}45/0_2]$

2.1 Experimental set-up

The low velocity impact was produced by an instrumented pendulum equipped with a piezoelectric load cell (PCB Piezotronics, Model 208A35) with semi-spherical head 12.7 mm in diameter which hit the middle of the tube in the orthogonal direction. The estimated impact energy was 7J, corresponding

to that of a small tool falling from about a meter, whereas the velocity was 3.5 m/s. Each tube was also instrumented by means of a couple of strain gauges (HBM LY41-6/350, 350 Ω, grid 6 mm), each connected in half bridge configuration with a heat compensator, in order to further investigate the evolution of the damage and its influence on mechanical properties.

The strain gauges were located at a distance of about 15 mm from the impact point, except in cases of impact on specimens with high torsional pre-load where they were positioned on the opposite side. The orientation of the grid was at ± 45º relative to the tube generatrix in order to acquire the deformation caused both by impact and torque.

The acquisition of the high speed signals (load and deformation) was made by a National Instruments board with a sampling frequency of 100 kHz. The tubes during the impact were blocked by a pair of grips to a torsional testing machine because the ultimate purpose was to measure the residual resistance to twisting after impact or to impose a torsional pre-load during impact.

Figure 1 shows the grasping system, consisting of four semi-cylindrical steel shells glued to the tube by a high resistance bi-component epoxy glue (Scotch-Weld 9323B / A 3M). The grips were appropriately shaped to transmit the torque and to reduce the stress concentration on the glue [11].
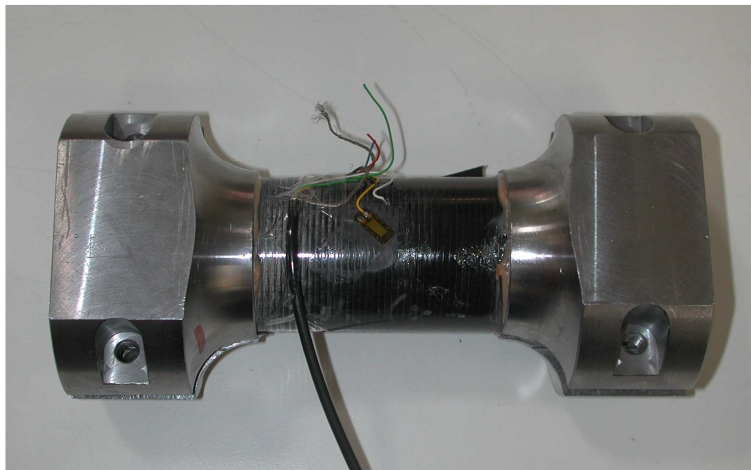

Figure 1: Tubular specimen with the grasping system.

Figure 2 shows the full experimental set-up, including: the Italsigma torsional testing machine, the instrumented pendulum and the signal acquisition system (torque, rotation, deformation of strain gauges, impact force and finally Acoustic Emission, whose details are not discussed in this paper).

The lateral impact tests were performed on specimens simply bound to the machine and on specimens pre-loaded in torsion (by controlling the displacement) with a torque equal to 65% or 130% of the torsional residual resistance (RRT) of not pre-loaded specimens.
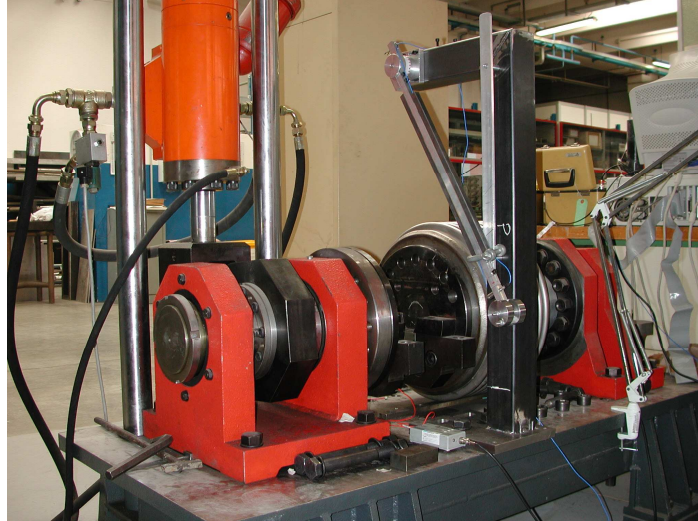
Figure 2: Experimental set-up.

2.2 Numerical model

The numerical modelling of CPS and QIS lamination sequences was performed using the finite element code ANSYS.

Solid185 Layered 8-node elements with three displacement degrees of freedom were used. Thus, by using the Layered option it was possible to define layer thickness and layer material direction angles as well as the orthotropic material properties shown in table 2. The load cell head was modeled as a rigid body and contact elements were placed close to the impacted area as shown in fig. 3. Sixteen elements 0.16mm thick were placed along the tube thickness (one for each lamina). A pure torque and a static lateral force, equal to the first peak load measured in the experimental test, were applied by placing them directly on pilot nodes. Furthermore, the analysis was performed in the condition of non-linear geometric behavior.

Table 2: Carbon/Epoxy elastic properties.

E_1	$E_2 = E_3$	$G_{12} = G_{13}$	G_{23}	$\nu_{12} = \nu_{13}$	ν_{23}
$105\ GPa$	$6.5\ GPa$	$5.5\ GPa$	$2.0\ GPa$	0.28	0.0256

As a failure criteria the 3-D Hashin-type [12] used in [2] was adopted and the values of matrix and fiber resistance, reported in table 3, were derived from the results of AE monitored torsion tests.

Table 3: Fiber and matrix resistance in tension,compression and shear.

σ_{FT}	σ_{FC}	σ_{MT}	σ_{MC}	τ_M
2390 MPa	$-1670\ MPa$	25 MPa	$-150\ MPa$	60 MPa

Since the static approximation was presumed to be valid and dynamic effects were ignored, fixed displacements and rotation of the free section of the tube were imposed as boundary conditions.
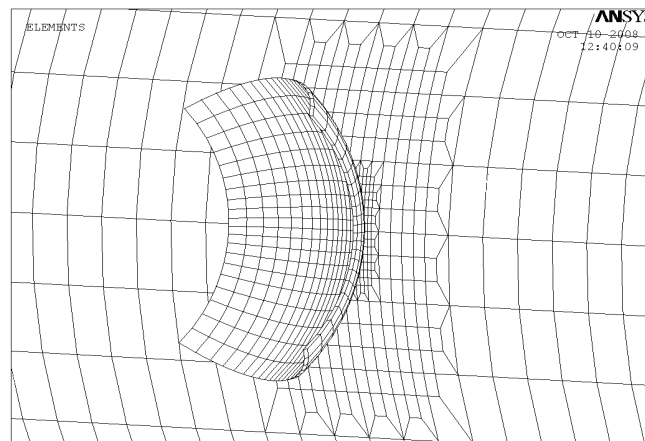

Figure 3: Model discretization.

3 Results

In Figure 4, the impact behaviors of the different lay-ups can be observed. The two quasi-isotropic sequences, QIS and QINS, had the same behavior, so only one trend was reported. In all three cases, a strongly accentuated initial peak followed by a fall, more pronounced for the cross ply specimens, can be noted.

A slowly growing load phase then follows, before the rebound of the impactor and the unloading of the specimen. The initial ascent phase represents the response of the undamaged material until the first failure, located at the beginning of the fall. The subsequent recovery of load was due to the global behavior of the structure that began to react when an greater impactor area came into contact with the material surface.

The impact damage was analogous in QI and CPS specimens while due to slightly greater damage the CPNS specimens reached lower load levels and longer impact duration.
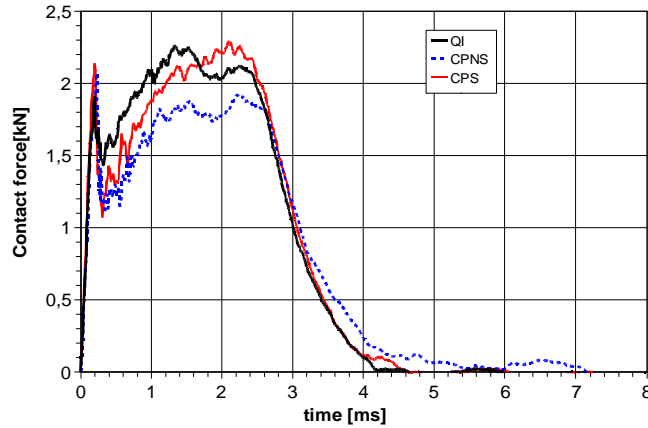
Figure 4: Effect of the lay-up on the impact load evolution.

Ignoring the difference in response due to the symmetry of the stacking sequences (only detectable in CP samples), Figures 5 and 6 report the contact force evolution versus time for the two configurations (QI and CP) having different torsional pre-load levels.

In the case of QI specimens it is possible to observe that the pre-load did not substantially change the response to impact, while the highest pre-load caused an elongation of the load fall phase with an increase of the overall duration of impact.
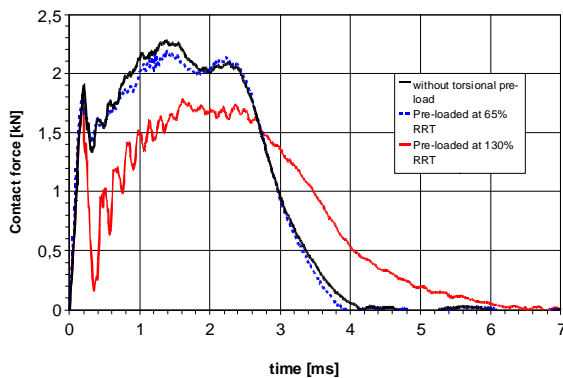

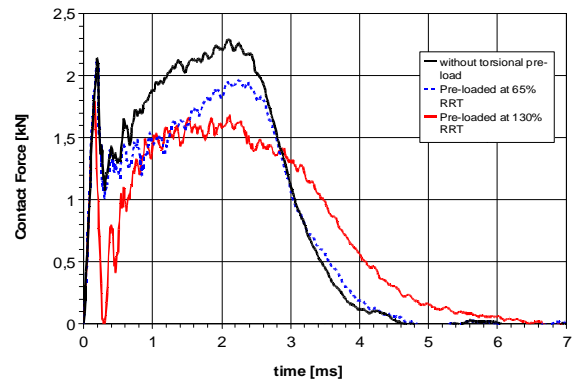Figure 5: Effect of the pre-load on QI specimens. Figure 6: Effect of the pre-load on CP specimens.

The behavior of CP tubes was different. In fact, the pre-load of 65% of RRT significantly changed the response; the load recovery after the first failure did not exceed the level reached by the first peak

as observed in the case of non pre-loaded specimens.

The impact on the pre-loaded tube at the highest level of torque provoked huge damage that led the first load to drop to zero. As in the case of QI specimens, the second load peak was significantly lower and the impact had a longer duration.

The strain gauge data made it possible to understand the mechanism of damage in more detail, albeit within the limits of local approach. Figures 7 to 9 show three representative examples of acquisition of strain trend during impacts. In the cases of high torsional pre-load when the gauges were glued near the point of impact, the gauge or the electrical connection braking always occurred in the earliest test phases. It was therefore decided to glue the gauge on the opposite side of the specimen.
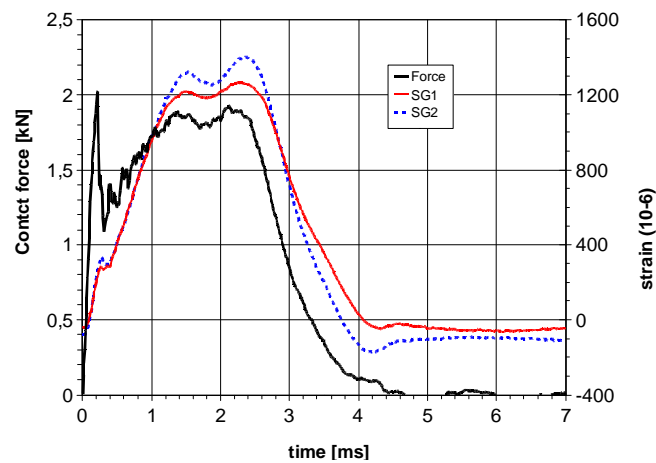

Figure 7: Strain in the presence of localized damage (CP not pre-loaded).

The key feature of all the readings is that the first peak load was detected barely or not at all.

On the contrary, in the subsequent phase of load recovery, in some cases, as in Figure 7, the deformation proportionally followed the trends of force, while in other cases, like that of Figure 8, the deformation followed the load up to a certain point, and then deviated significantly .

This behavior can certainly be related to the progression of delamination; in fact, when the strain ceases to be proportional to the load it can be reasonably due to the delamination front passing under the strain gauges.

In Figure 9 it is possible to see the overall effect in a highly pre-loaded specimen. In this case, the gauges, placed at 45° relative to the cylinder generatrix, and perpendicular to each other, due to the impact and with a slight delay of 200 microseconds, are downloaded near to zero, showing the relaxation of the pre-load.

The visual inspection of the damaged zones showed clear differences both in stacking sequence (between QI and CP, while there were no noticeable differences due to the presence or absence of symmetry) and as regards the effect of pre-load.
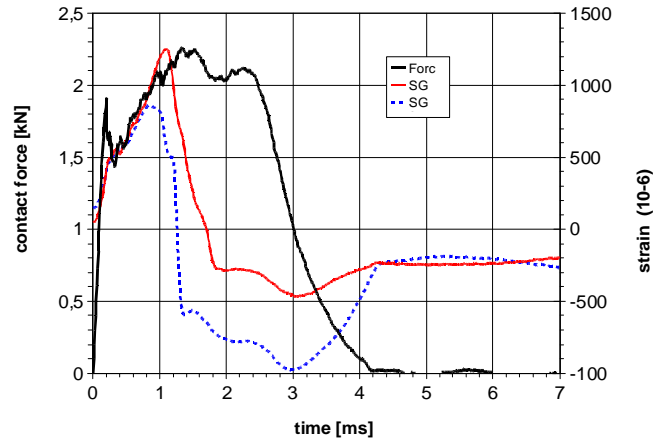
Figure 8: Strain in the presence of delamination (QI not pre-loaded).
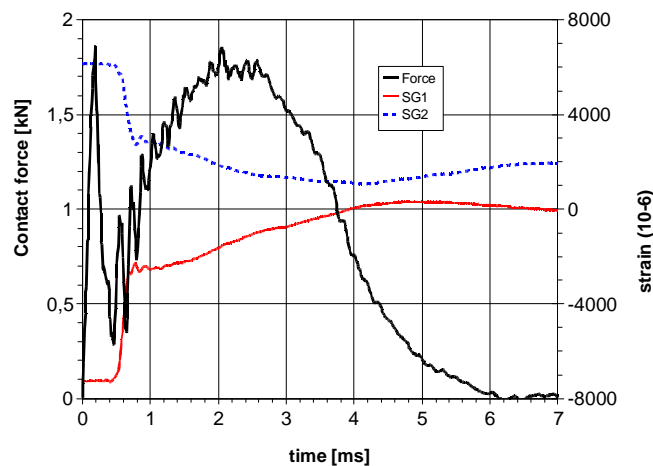

Figure 9: Strain in highly damaged specimen (QI pre-loaded at 130% RRT, strain gages far from the impact point).

Figure 10 shows the macroscopic effects of impact on not pre-loaded specimens on the outer surface and on the correspondent inner surface. In QI specimens, the damage produced is barely visible outside (Figure 10A) with a slight dent, small matrix cracks and some fiber cracking. Inside (Figure 10B), we see instead a small swelling due to delamination, sometimes accompanied by a slight splitting. In the CP samples signs of splitting are visible on the external lamina (Figure 10C) around the impact mark (Figure 10D) and on the external ply just below the impact point.

The effects of the pre-load on test are shown in Figure 11. In this case we have only the image of the exterior of the tube after the collision because the samples were immediately broken in torsion without releasing the pre-load and this made it impossible to document the damage on the inner face.

The QI tubes pre-loaded to 65% of RRT (Figure 11A) showed a marked imprint, clearly visible, and the detachment of the 0º external lamina, fractured in the direction perpendicular to the fibers.

The QI specimens pre-loaded at 130% of the RRT (Figure 11B) experienced a marked breakdown of the internal plies that led to the detachment of the external lamina in several places (without breaking the fibers placed at 0º).
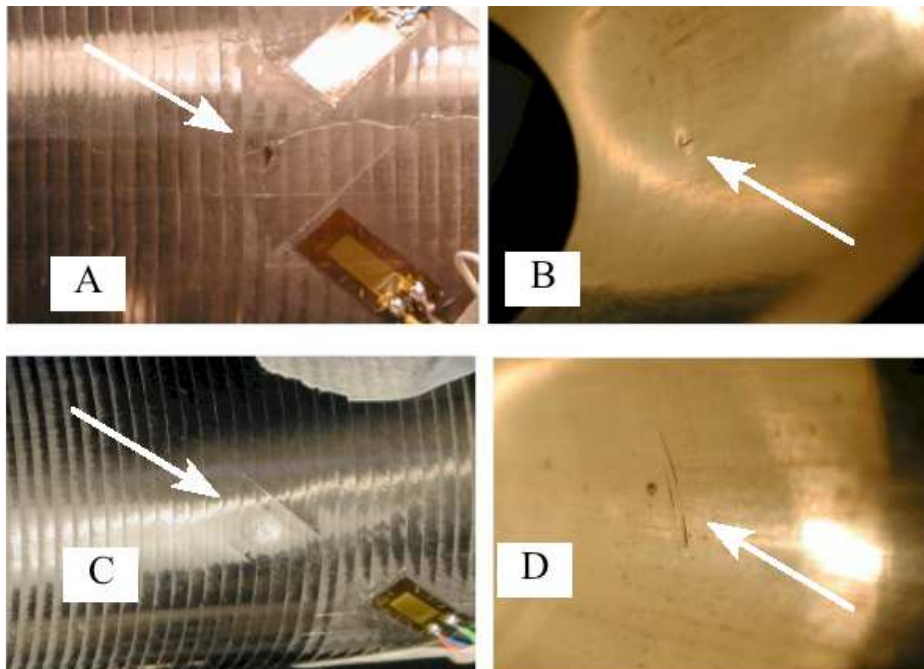

Figure 10: Damage of not pre-loaded specimens QI ((A) inner surface, (B) outer s.) and CP ((C) outer s., (D) inner s.).

In CP samples at the lowest level of pre-load (Figure 11C), a hollow centered at the point of impact and oriented to 45º was produced. Finally, in the tubes pre-loaded at the highest level of torque (Figure 11D) the hollow became a twisted fracture that affected the entire length of the tube as far as the grips and, as seen by rotating in the opposite direction to the one that caused the initial pre-load, crossed the whole thickness.
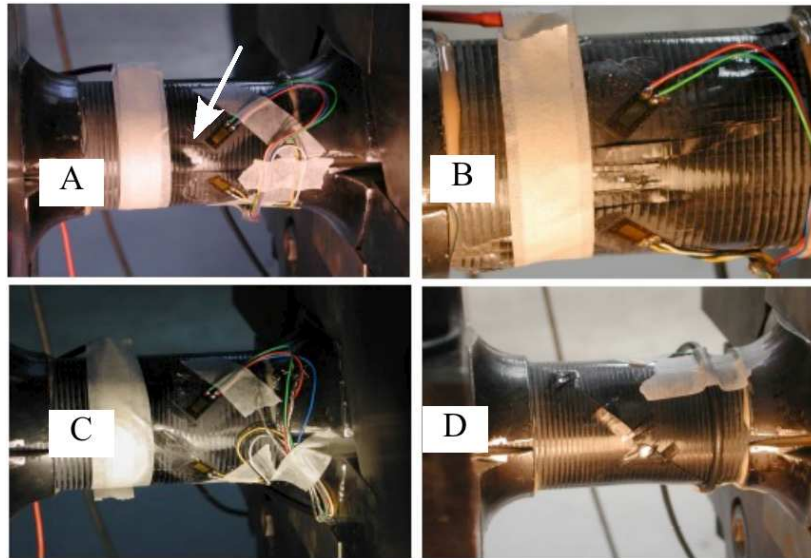
Figure 11: Damage of pre-loaded specimens (A) QI 65% RRT, (B) QI 130% RRT, (C) CP 65% RRT, (D) CP 130%RRT.

The following four figures show results of numerical simulations in terms of contour plots of the Hashin criterion for fiber and matrix failure. In particular, two different layups for the outermost ply and for the internal one are considered.

The square area represented in the figures has a dimension of $15 \times 15 \text{mm}^2$ and is centered in the contact point. The plots relative to the three levels of pre-load are shown.

In figures 12 and 13 fiber failure is considered respectively for QI and CP specimens. The damage index value and the dimension of the damaged area are independent of (for QI) or slightly dependent (for CP) on the torsional preload. In both cases, the fiber failure condition is obtained in the outermost lamina.

The matrix damage index contours are shown in Figure 13 for QI and in Figure 14 for CP specimens.

From these index contour maps it is possible to see that the inner lamina had a larger matrix damaged area than the external one and it increased for higher pre-loads, while in the case of CP tubes the damaged area of the external ply was independent of the pre-load.

In all cases, the matrix damage index indicated the presence of matrix cracking that is the origin of delamination in the case of components with high flexural stiffness, like the tubes [13].
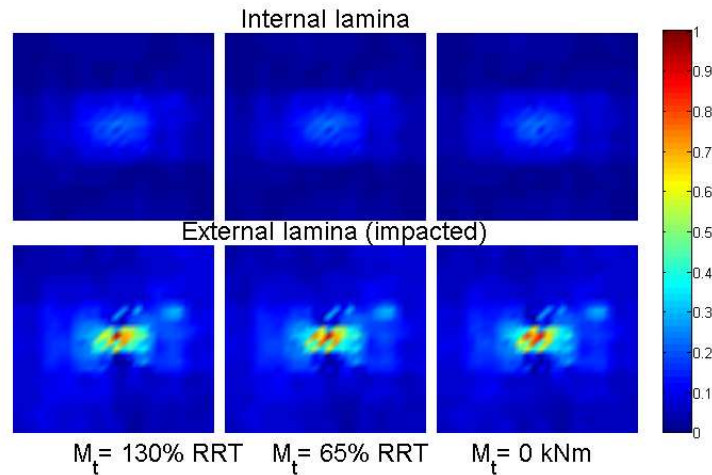
Internal lamina

External lamina (impacted)

$M_t = 130\%$ RRT $M_t = 65\%$ RRT $M_t = 0$ kNm

Figure 12: Hashin Criterion for fiber failure in QI lay-up.

Internal lamina

External lamina (impacted)
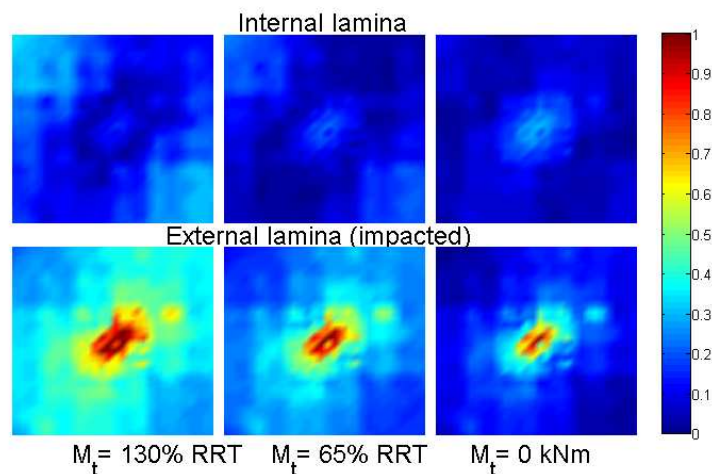
$M_t = 130\%$ RRT $M_t = 65\%$ RRT $M_t = 0$ kNm

Figure 13: Hashin Criterion for fiber failure in CP lay-up.

4 Discussion

The measures of contact force and deformation during the impact, together with the observation of the specimens after testing and with the numerical simulations, suggest some considerations about the effects of the lay-up and of the level of torsional pre-load on the impact behavior and in particular on the mechanisms of fracture.
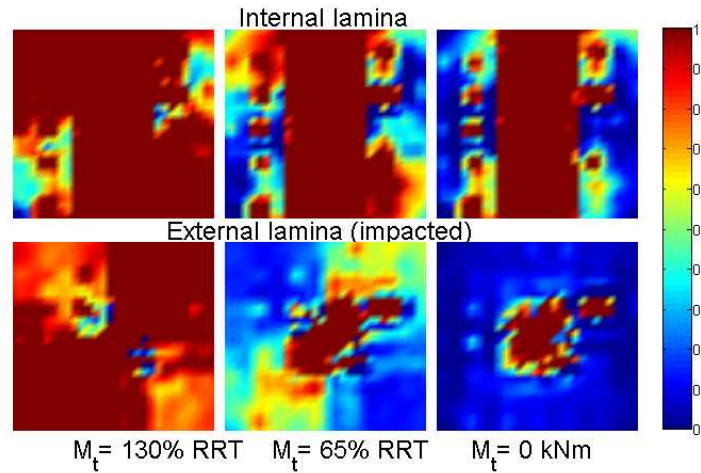
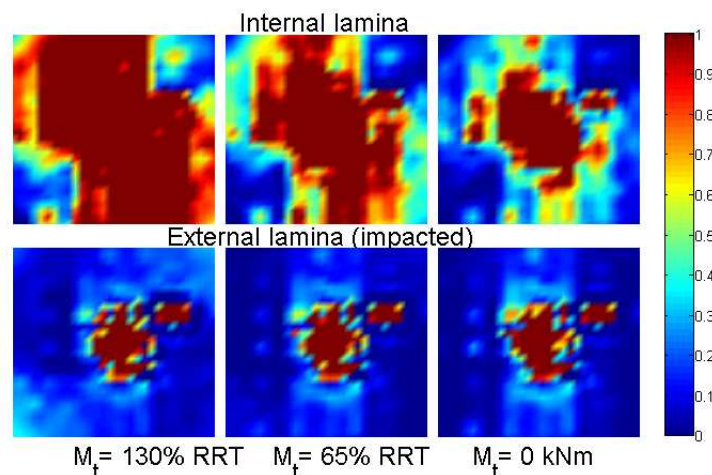Figure 14: Hashin Criterion for matrix failure in QI lay-up.

Figure 15: Hashin Criterion for matrix failure in CP lay-up.

As regards the QI tubes, no difference in impact behavior between QIS and QINS was noted, and this is not surprising since this is a flexural problem in which the external 0° fiber stiffness tends to prevail [8]. On the contrary, in the CP specimens it was possible to note the effect of the succession of the different interfaces present in the CPNS tubes compared with the CPS ones (Fig. 4).

In general, the torsional pre-load role was to provide a certain amount of strain energy available for the propagation of the initial damage provoked by the impact. The response in the early moments

did not change compared to the case without pre-load and the maximum load reached was the same; from that point onwards, the trends were different because of the different evolution of damage. From the value of force measured in the second peak and from the visual inspection it can be deduced that the QI specimens were less damaged than the CP ones in this particular loading condition (Figs. 5 and 6).

Turning to the mechanisms of fracture, without doubt the matrix fracture and delamination were present and in some cases it was possible to see failure of the fibers on the outer ply with the naked eye. The peak of force (and the next fall) highlighted in the very first moments of all the impact tests did not match a similar trend of the deformation acquired by the strain gauges, which at most showed only slight discontinuity or change of slope. Only in the following phases were the readings of the gauges consistent with the reading of the load cell. This means that the initial material damage caused by the first peak load occurred in the early stages in a small area adjacent to the point of impact, at a shorter distance than the one between the point of impact and the strain gauges (which was about 15 mm).

This interpretation is confirmed by the numerical model; in fact, for both lay-ups, the fibers and the matrix of the external ply, on which the strain gauges were glued, were considered broken in a small area around the contact point, according to the Hashin criterion (see Figs 12-15).

Due to this localized failure the amplitude of the elastic wave that reached the gauges was significantly lower than what could be expected considering the value of the peak load. In the following few instants the impactor came into contact with larger parts of the laminate so the extent of deformation increased due to the global flexural behavior.

It is likely that the first load drop was provoked by delamination, induced by the first matrix failure visible on the outer surface [13] and foreseen also by the numerical model (see Figs. 14,15).

The delamination continued to spread even further, as shown by some of the measures of the strain gauges (Fig.8) where a rapid change of the strain trend can be noted. This strain trend variation can be explained as a consequence of delaminations between the external ply, over which the sensor is placed, and the rest of the laminate

Among other things, this observation confirms that, as usually happens in CFRP laminates, the inner impact damage is much more extensive than visual inspection may show.

Summarizing, the failure mechanism started with the matrix breakage in the contact area; this originated the delamination onset and growth at least under the outer lamina. The inner lamina also showed delamination and it was probably spread all through the thickness. In the pre-loaded specimens delamination induced the buckling of the laminas in compression and finally also the laminas in tension failed due to overstress.

5 Conclusion

The effects of the lay-up and of the level of torsional pre-load on the response of composite tubes under impact were studied.

The experimental testing and the numerical modelling showed that:

1. in all cases the impact damage is highly localized as regards fiber failure, while delamination and matrix cracking are spread through the thickness;
2. the QI specimens were less damaged than the CP ones and among these the CPS specimens have a slightly better behavior than CPNS samples while there is no difference between QIS and QINS specimens.
3. the presence of the torsional pre-load significantly changed the elastic response and increased the amount of damage, especially in the case of CP samples, in some cases up to complete breakage of the specimen.

Acknowledgements

References

[1] Abrate, S., *Impact on composite structures*. Cambridge University Press: New York, 1998.
[2] Cesari, F., Dal Re, V., Minak, G. & Zucchelli, A., Damage and residual strength of laminated carbon-epoxy composite circular plates loaded at the centre. *Composites Part A: Applied Science and Manufacturing*, **38(4)**, pp. 1163–1173, 2006.
[3] Minak, G., Morelli, P. & Zucchelli, A., Fatigue residual strength of laminated graphite-epoxy composite circular plates damaged by transversal loads. *Composite Science and Technology*, 2008. In Press 10.1016/j.compscitech.2008.05.025.
[4] Minak, G. & Ghelli, D., Influence of diameter and boundary conditions on low velocity impact response of CFRP circular laminated plates. *Composites Part B: Engineering*, **39**, pp. 962–972, 2008.
[5] Christoforou, A.P., Swanson, S.R. & Beckwith, S.W., Lateral impact of composite cylinders. *Composite Materials: Fatigue and Fracture*, **2(ASTM STP 1012)**, pp. 373–386, 1989.
[6] Christoforou, A.P. & Swanson, S.R., Analysis of simply-supported orthotropic cylindrical shells subject to lateral impact loads. *Transactions of the ASME*, **57**, p. 376, 1990.
[7] Krishnamurthy, K.S., Mahajan, P. & Mittal, R.K., A parametric study of the impact response and damage of laminated cylindrical composite shells. *Composites Science and Technology*, **61**, pp. 1655–1669, 2001.
[8] Kim, S.J., Goo, N.S. & Kim, T.W., The effect of curvature on the dynamic response and impact-induced damage in composite laminates. *Composites Science and Technology*, **51**, pp. 763–773, 1997.
[9] Her, S.C. & Liang, Y.C., The finite element analysis of composite laminates and shell structures subjected to low velocity impact. *Composite Structures*, **66**, pp. 277–285, 2004.
[10] Doyum, A.B. & Altay, U.B., Low-velocity impact damage in glass fibre/epoxy cylindrical tubes. *Materials & Design*, **18(3)**, pp. 131–135, 1997.
[11] Minak, G., Ghelli, D. & Zucchelli, A., Torsion testing of cfrp laminate tubes. *5th ESIS TC4 International Conference on Fracture of Polymers, Composites and Adhesives*, Les Diablerets, 2008.
[12] Hashin, Z., Failure criteria for unidirectional composites. *J Appl Mech*, **47**, pp. 329–334, 1980.
[13] Abrate, S., Impact on laminated composite materials. *Appl Mech Rev*, **44(4)**, pp. 155–190, 1991.